

Relic Gravitational Waves and Their Detection

L. P. Grishchuk*

*Department of Physics and Astronomy, Cardiff University, Cardiff CF2 3YB, United Kingdom
and*

Sternberg Astronomical Institute, Moscow University, Moscow 119899, Russia

The range of expected amplitudes and spectral slopes of relic (squeezed) gravitational waves, predicted by theory and partially supported by observations, is within the reach of sensitive gravity-wave detectors. In the most favorable case, the detection of relic gravitational waves can be achieved by the cross-correlation of outputs of the initial laser interferometers in LIGO, VIRGO, GEO600. In the more realistic case, the sensitivity of advanced ground-based and space-based laser interferometers will be needed. The specific statistical signature of relic gravitational waves, associated with the phenomenon of squeezing, is a potential reserve for further improvement of the signal to noise ratio.

I. INTRODUCTION

It is appropriate and timely to discuss the detection of relic gravitational waves at the experimental meeting like this one. We are in the situation when the advanced laser interferometers, currently under construction or in a design phase, can make the dream of detecting relic gravitons a reality. The detection of relic gravitational waves is the only way to learn about the evolution of the very early Universe, up to the limits of Planck era and Big Bang.

The existence of relic gravitational waves is a consequence of quite general assumptions. Essentially, we rely only on the validity of general relativity and basic principles of quantum field theory. The strong variable gravitational field of the early Universe amplifies the inevitable zero-point quantum oscillations of the gravitational waves and produces a stochastic background of relic gravitational waves measurable today [1]. It is important to appreciate the fundamental and unavoidable nature of this mechanism. Other physical processes can also generate stochastic backgrounds of gravitational waves. But those processes either involve many additional hypotheses, which may turn out to be not true, or produce a gravitational wave background (like the one from binary stars in the Galaxy) which should

*e-mail: grishchuk@astro.cf.ac.uk

be treated as an unwanted noise rather than a useful and interesting signal. The scientific importance of detecting relic gravitational waves has been stressed on several occasions (see, for example, [2]– [4]).

The central notion in the theory of relic gravitons is the phenomenon of superadiabatic (parametric) amplification. The roots of this phenomenon are known in classical physics, and we will remind its basic features. As every wave-like process, gravitational waves use the concept of a harmonic oscillator. The fundamental equation for a free harmonic oscillator is

$$\ddot{q} + \omega^2 q = 0, \quad (1)$$

where q can be a displacement of a mechanical pendulum or a time-dependent amplitude of a mode of the physical field. The energy of the oscillator can be changed by an acting force or, alternatively, by a parametric influence, that is, when a parameter of the oscillator, for instance the length of a pendulum, is being changed. In the first case, the fundamental equation takes the form

$$\ddot{q} + \omega^2 q = f(t), \quad (2)$$

whereas in the second case Eq. (1) takes the form

$$\ddot{q} + \omega^2(t)q = 0. \quad (3)$$

Equations (2) and (3) are profoundly different, both, mathematically and physically.

Let us concentrate on the parametric influence. We consider a pendulum of length L oscillating in a constant gravitational field g . The unperturbed pendulum oscillates with the constant frequency $\omega = \sqrt{g/L}$. *Fig.1a* illustrates the variation of the length of the pendulum $L(t)$ by an external agent, shown by alternating arrows. Since $L(t)$ varies, the frequency of the oscillator does also vary: $\omega(t) = \sqrt{g/L(t)}$. The variation $L(t)$ does not need to be periodic, but cannot be too much slow (adiabatic) if the result of the process is going to be significant. Otherwise, in the adiabatic regime of slow variations, the energy of the oscillator E and its frequency ω do change slowly, but E/ω remains constant, so one can say that the “number of quanta” $E/\hbar\omega$ in the oscillator remains fixed. In other words, for the creation of new “particles - excitations”, the characteristic time of the variation should be comparable with the period of the oscillator and the adiabatic behaviour should be violated. After some duration of the appropriate parametric influence, the pendulum will oscillate at the original frequency, but will have a significantly larger, than before, amplitude and energy. This is shown in *Fig.1b*. Obviously, the energy of the oscillator has been increased at the expense of the external agent (pump field). For simplicity, we have considered a familiar case, when the length of the pendulum varies, while the gravitational acceleration g remains constant. Variation of g would represent a gravitational parametric influence and would be even in a closer analogy with what we study below.

A classical oscillator must have a non-zero initial amplitude for the amplification mechanism to work. Otherwise, if the initial amplitude is zero, the final amplitude will also be zero. Indeed, imagine the pendulum strictly at rest, hanging stright down. Whatever the variation of its length is, it will not make the pendulum to oscillate and gain energy. In contrast, a quantum oscillator does not need to be excited from the very beginning. The oscillator can be initially in its vacuum quantum-mechanical state. The inevitable zero-point

quantum oscillations are associated with the vacuum state energy $\frac{1}{2}\hbar\omega$. One can imagine a pendulum hanging stright down, but fluctuating with a tiny amplitude determined by the “half of the quantum in the mode”. In the classical picture, it is this tiny amplitude of quantum-mechanical origin that is being parametrically amplified.

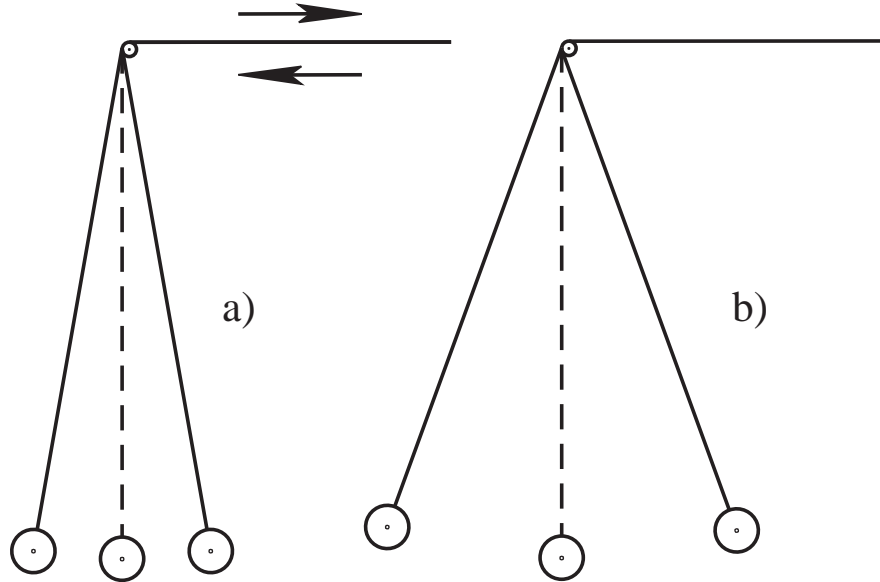


Fig. 1. Parametric amplification. a) variation of the length of the pendulum, b) increased amplitude of oscillations.

The Schrodinger evolution of a quantum oscillator depends crucially on whether the oscillator is being excited parametrically or by a force. Consider the phase diagram (q, p) , where q is the displacement and p is the conjugate momentum. The vacuum state is described by the circle in the center (see *Fig.2*). The mean values of q and p are zeros, but their variances (zero-point quantum fluctuations) are not zeros and are equal to each other. Their numerical values are represented by the circle in the center. Under the action of a force, the vacuum state evolves into a coherent state. The mean values of p and q have increased, but the variances are still equal and are described by the circle of the same size as for the vacuum state. On the other hand, under a parametric influence, the vacuum state evolves into a squeezed vacuum state. [For a recent review of squeezed states see, for example, [5] and references there.] Its variances for the conjugate variables q and p are significantly unequal and are described by an ellipse. As a function of time, the ellipse rotates with respect to the origin of the (q, p) diagram, and the numerical values of the variances oscillate too. The mean numbers of quanta in the two states, one of which is coherent and another is squeezed vacuum, can be equal (similar to the coherent and squeezed states shown in *Fig.2*) but the statistical properties of these states are significantly different. Among other things, the variance of the phase of the oscillator in a squeezed vacuum state is very small (squeezed). Graphically, this is reflected in the fact that the ellipse is very thin, so that that the uncertainty in the angle between the horizontal axis and the orientation of the ellipse is

very small. This highly elongated ellipse can be regarded as a portrait of the gravitational wave quantum state that is being inevitably generated by parametric amplification, and which we will be dealing with below.

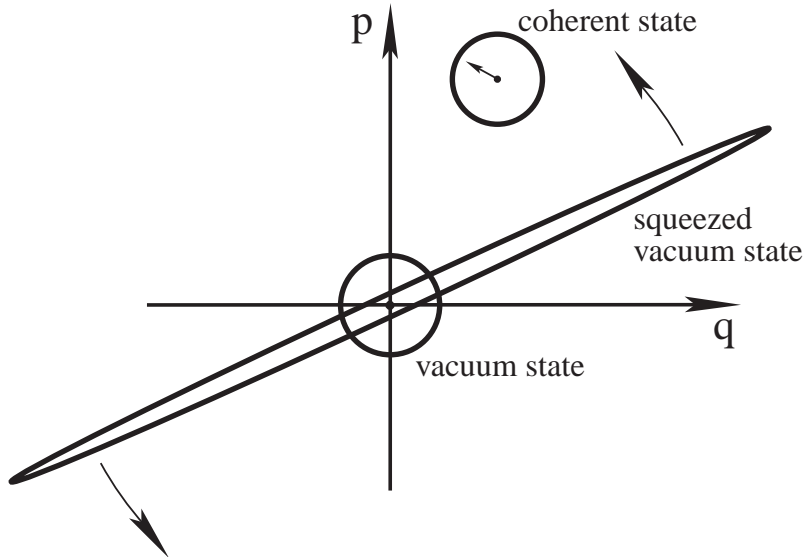


Fig. 2. Some quantum states of a harmonic oscillator.

A wave-field is not a single oscillator, it depends on spatial coordinates and time, and may have several independent components (polarization states). However, the field can be decomposed into a set of spatial Fourier harmonics. In this way we represent the gravitational wave field as a collection of many modes, many oscillators. Because of the nonlinear character of the Einstein equations, each of these oscillators is coupled to the variable gravitational field of the surrounding Universe. For sufficiently short gravitational waves of experimental interest, this coupling was especially effective in the early Universe, when the condition of the adiabatic behaviour of the oscillator was violated. It is this homogeneous and isotropic gravitational field of all the matter in the early Universe that played the role of the external agent - pump field. The variable pump field acts parametrically on the gravity-wave oscillators and drives them into multiparticle states. Concretely, the initial vacuum state of each pair of waves with oppositely directed momenta evolves into a highly correlated state known as the two-mode squeezed vacuum state [6], [7]. The strength and duration of the effective coupling depends on the oscillator's frequency. They all start in the vacuum state but get excited to various amounts. As a result, a broad spectrum of relic gravitational waves is being formed. This spectrum is accessible to our observations today.

Let us formulate the problem in more detail.

II. COSMOLOGICAL GRAVITATIONAL WAVES

In the framework of general relativity, a homogeneous isotropic gravitational field is described by the line element

$$ds^2 = c^2 dt^2 - a^2(t) \delta_{ij} dx^i dx^j = a^2(\eta) [d\eta^2 - \delta_{ij} dx^i dx^j]. \quad (4)$$

In cosmology, the function $a(t)$ (or $a(\eta)$) is called scale factor. In our discussion, it will represent gravitational pump field.

Cosmological gravitational waves are small corrections h_{ij} to the metric tensor. They are defined by the expression

$$ds^2 = a^2(\eta) [d\eta^2 - (\delta_{ij} + h_{ij}) dx^i dx^j]. \quad (5)$$

The functions $h_{ij}(\eta, \mathbf{x})$ can be expanded over spatial Fourier harmonics $e^{i\mathbf{n}\mathbf{x}}$ and $e^{-i\mathbf{n}\mathbf{x}}$, where \mathbf{n} is a constant wave vector. In this way, we reduce the dynamical problem to the evolution of time-dependent amplitudes for each mode \mathbf{n} . Among six functions h_{ij} there are only two independent (polarization) components. This decomposition can be made, both, for real and for quantized field h_{ij} . In the quantum version, the functions h_{ij} are treated as quantum-mechanical operators. We will use the Heisenberg picture in which the time evolution is carried out by the operators while the quantum state is fixed. This picture is fully equivalent to the Schrodinger picture, discussed in the Introduction, in which the vacuum state evolves into a squeezed vacuum state while the operators are time independent.

The Heisenberg operator for the quantized real field h_{ij} can be written as

$$h_{ij}(\eta, \mathbf{x}) = \frac{C}{(2\pi)^{3/2}} \int_{-\infty}^{\infty} d^3\mathbf{n} \sum_{s=1}^2 \overset{s}{p}_{ij}(\mathbf{n}) \frac{1}{\sqrt{2n}} \left[\overset{s}{h}_n(\eta) e^{i\mathbf{n}\mathbf{x}} \overset{s}{c}_{\mathbf{n}} + \overset{s}{h}_n^*(\eta) e^{-i\mathbf{n}\mathbf{x}} \overset{s}{c}_{\mathbf{n}}^\dagger \right], \quad (6)$$

where C is a constant which will be discussed later. The creation and annihilation operators satisfy the conditions $[\overset{s'}{c}_{\mathbf{n}}, \overset{s}{c}_{\mathbf{m}}^\dagger] = \delta_{s's} \delta^3(\mathbf{n} - \mathbf{m})$, $\overset{s}{c}_{\mathbf{n}}|0\rangle = 0$, where $|0\rangle$ (for each \mathbf{n} and s) is the fixed initial vacuum state discussed below. The wave number n is related with the wave vector \mathbf{n} by $n = (\delta_{ij} n^i n^j)^{1/2}$. The two polarization tensors $\overset{s}{p}_{ij}(\mathbf{n})$ ($s = 1, 2$) obey the conditions

$$\overset{s}{p}_{ij} n^j = 0, \quad \overset{s}{p}_{ij} \delta^{ij} = 0, \quad \overset{s'}{p}_{ij} \overset{s}{p}{}^{ij} = 2\delta_{ss'}, \quad \overset{s}{p}_{ij}(-\mathbf{n}) = \overset{s}{p}_{ij}(\mathbf{n}).$$

The time evolution, one and the same for all \mathbf{n} belonging to a given n , is represented by the complex time-dependent function $\overset{s}{h}_n(\eta)$. This evolution is dictated by the Einstein equations. The nonlinear nature of the Einstein equations leads to the coupling of $\overset{s}{h}_n(\eta)$ with the pump field $a(\eta)$. For every wave number n and each polarization component s , the functions $\overset{s}{h}_n(\eta)$ have the form

$$\overset{s}{h}_n(\eta) = \frac{1}{a(\eta)} [\overset{s}{u}_n(\eta) + \overset{s}{v}_n^*(\eta)], \quad (7)$$

where $\overset{s}{u}_n(\eta)$ and $\overset{s}{v}_n(\eta)$ can be expressed in terms of the three real functions (the polarization index s is omitted): r_n - squeeze parameter, ϕ_n - squeeze angle, θ_n - rotation angle,

$$u_n = e^{i\theta_n} \cosh r_n, \quad v_n = e^{-i(\theta_n - 2\phi_n)} \sinh r_n. \quad (8)$$

The dynamical equations for $u_n(\eta)$ and $v_n(\eta)$

$$i\frac{du_n}{d\eta} = nu_n + i\frac{a'}{a}v_n^*, \quad i\frac{dv_n}{d\eta} = nv_n + i\frac{a'}{a}u_n^* \quad (9)$$

lead to the dynamical equations governing the functions $r_n(\eta)$, $\phi_n(\eta)$, $\theta_n(\eta)$ [7]:

$$r'_n = \frac{a'}{a} \cos 2\phi_n, \quad \phi'_n = -n - \frac{a'}{a} \sin 2\phi_n \coth 2r_n, \quad \theta'_n = -n - \frac{a'}{a} \sin 2\phi_n \tanh r_n, \quad (10)$$

where $' = d/d\eta$, and the evolution begins from $r_n = 0$. This value of r_n characterizes the initial vacuum state $|0\rangle$ which is defined long before the interaction with the pump field became effective, that is, long before the coupling term a'/a became comparable with n . The constant C should be taken as $C = \sqrt{16\pi} l_{Pl}$ where $l_{Pl} = (G\hbar/c^3)^{1/2}$ is the Planck length. This particular value of the constant C guarantees the correct quantum normalization of the field: energy $\frac{1}{2}\hbar\omega$ per each mode in the initial vacuum state. The dynamical equations and their solutions are identical for both polarization components s .

Equations (9) can be translated into the more familiar form of the second-order differential equation for the function $\dot{\mu}_n(\eta) \equiv \dot{u}_n(\eta) + \dot{v}_n^*(\eta) \equiv a(\eta)\dot{h}_n(\eta)$ [1]:

$$\mu_n'' + \mu_n \left[n^2 - \frac{a''}{a} \right] = 0. \quad (11)$$

Clearly, this is the equation for a parametrically disturbed oscillator (compare with Eq. (3)). In absence of the gravitational parametric influence represented by the term a''/a , the frequency of the oscillator defined in terms of η -time would be a constant: n . Whenever the term a''/a can be neglected, the general solution to Eq. (11) has the usual oscillatory form

$$\mu_n(\eta) = A_n e^{-inn\eta} + B_n e^{inn\eta}, \quad (12)$$

where the constants A_n , B_n are determined by the initial conditions. On the other hand, whenever the term a''/a is dominant, the general solution to Eq. (11) has the form

$$\mu_n(\eta) = C_n a + D_n a \int^\eta \frac{d\eta}{a^2}. \quad (13)$$

In fact, this approximate solution is valid as long as n is small in comparison with $|a'/a|$. This is more clearly seen from the equivalent form of Eq. (11) written in terms of the function $h_n(\eta)$ [8]:

$$h_n'' + 2\frac{a'}{a}h_n' + n^2 h_n = 0. \quad (14)$$

For growing functions $a(\eta)$, that is, in expanding universes, the second term in Eq.(13) is usually smaller than the first one (see below), so that, as long as $n \ll a'/a$, the dominant solution is the growing function $\mu_n(\eta) = C_n a(\eta)$, and

$$h_n = \text{const.} \quad (15)$$

Equation (11) can be also looked at as a kind of the Schrodinger equation for a particle moving in presence of the effective potential $U(\eta) = a''/a$. In the situations that are normally

considered, the potential $U(\eta)$ has a bell-like shape and forms a barrier (see *Fig.3*). When a given mode n is outside the barrier, its amplitude h_n is adiabatically decreasing with time: $h_n \propto \frac{e^{\pm i n \eta}}{a(\eta)}$. This is shown in *Fig.3* by oscillating lines with decreasing amplitudes of oscillations. The modes with sufficiently high frequencies do not interact with the barrier, they stay above the barrier. Their amplitudes h_n behave adiabatically all the time. For these high-frequency modes, the initial vacuum state (in the Schrodinger picture) remains the vacuum forever. On the other hand, the modes that interact with the barrier are subject to the superadiabatic amplification. Under the barrier and as long as $n < a'/a$, the function h_n stays constant instead of the adiabatic decrease. For these modes, the initial vacuum state evolves into a squeezed vacuum state.

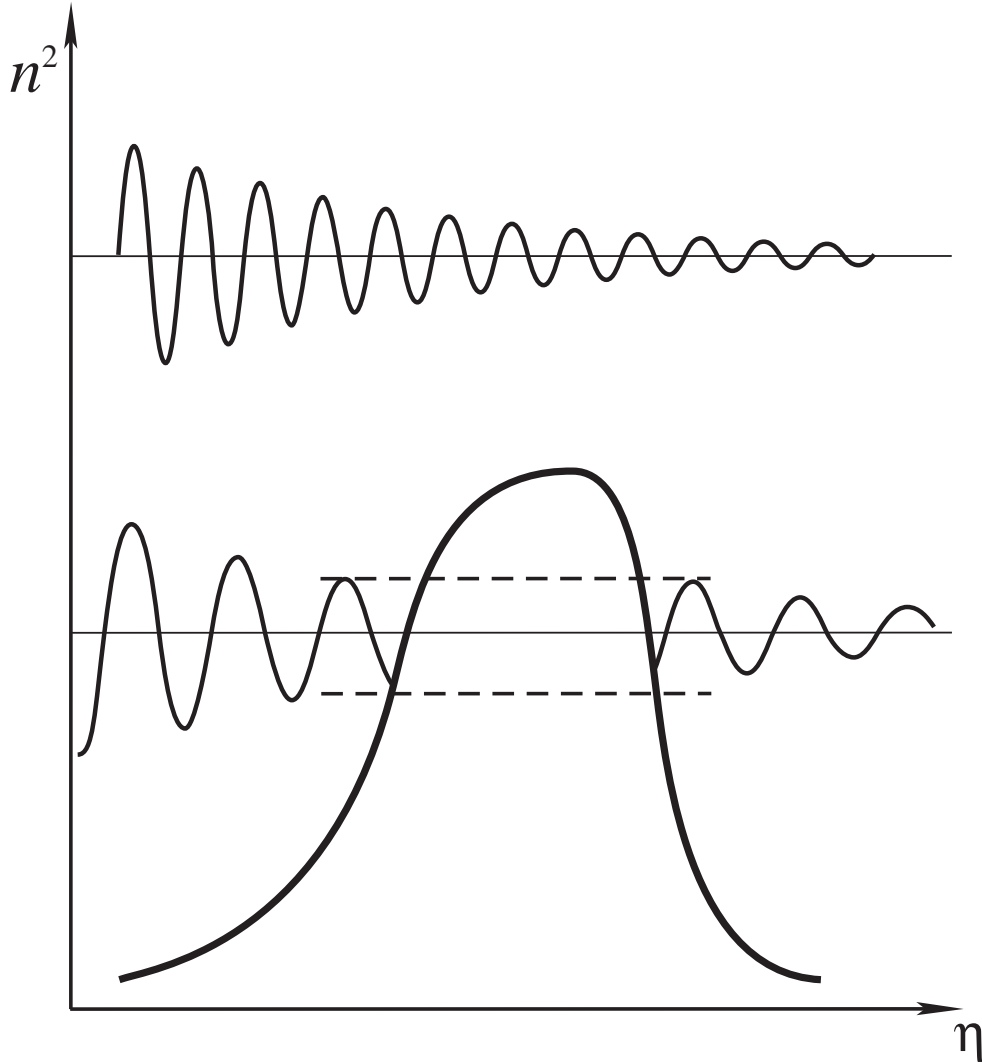


Fig. 3. Effective potential $U(\eta)$.

After having formulated the initial conditions, the present day behaviour of r_n, ϕ_n, θ_n (or, equivalently, the present day behaviour of h_n) is essentially all we need to find. The mean number of particles in a two-mode squeezed state is $2 \sinh^2 r_n$ for each s . This number

determines the mean square amplitude of the gravitational wave field. The time behaviour of the squeeze angle ϕ_n determines the time dependence of the correlation functions of the field. The amplification (that is, the growth of r_n) governed by Eq. (10) is different for different wave numbers n . Therefore, the present day results depend on the present day frequency ν ($\nu = cn/2\pi a$) measured in $H z$.

In cosmology, the function $H \equiv \dot{a}/a \equiv ca'/a^2$ is the time-dependent Hubble parameter. The function $l \equiv c/H$ is the time-dependent Hubble radius. The time-dependent wavelength of the mode n is $\lambda = 2\pi a/n$. The wavelength λ has this universal definition in all regimes. In contrast, the ν defined as $\nu = cn/2\pi a$ has the usual meaning of a frequency of an oscillating process only in the short-wavelength (high-frequency) regime of the mode n , that is, in the regime where $\lambda \ll l$. As we have seen above, the qualitative behaviour of solutions to Eqs. (11), (14) depends crucially on the comparative values of n and a'/a , or, in other words, on the comparative values of $\lambda(\eta)$ and $l(\eta)$. This relationship is also crucial for solutions to Eq. (10) as we shall see now.

In the short-wavelength regime, that is, during intervals of time when the wavelength $\lambda(\eta)$ is shorter than the Hubble radius $l(\eta) = a^2/a'$, the term n in (10) is dominant. The functions $\phi_n(\eta)$ and $\theta_n(\eta)$ are $\phi_n = -n(\eta + \eta_n)$, $\theta_n = \phi_n$ where η_n is a constant. The factor $\cos 2\phi_n$ is a quickly oscillating function of time, so the squeeze parameter r_n stays practically constant. This is the adiabatic regime for a given mode.

In the opposite, long-wavelength regime, the term n can be neglected. The function ϕ_n is $\tan \phi_n(\eta) \approx \text{const}/a^2(\eta)$, and the squeeze angle quickly approaches one of the two values: $\phi_n = 0$ or $\phi_n = \pi$ (analog of “phase bifurcation” [9]). The squeeze parameter $r_n(\eta)$ grows with time according to

$$r_n(\eta) \approx \ln \frac{a(\eta)}{a_*}, \quad (16)$$

where a_* is the value of $a(\eta)$ at η_* , when the long-wavelength regime, for a given n , begins. The final amount of r_n is

$$r_n \approx \ln \frac{a_{**}}{a_*}, \quad (17)$$

where a_{**} is the value of $a(\eta)$ at η_{**} , when the long-wavelength regime and amplification come to the end. It is important to emphasize that it is not a “sudden transition” from one cosmological era to another that is responsible for amplification, but the entire interval of the long-wavelength (non-adiabatic) regime.

After the end of amplification, the accumulated (and typically large) squeeze parameter r_n stays approximately constant. The mode is again in the adiabatic regime. In course of the evolution, the complex functions $u_n^s(\eta) + v_n^{s*}(\eta)$ become practically real, and one has $h_n^s(\eta) \approx h_n^{s*}(\eta) \approx \frac{1}{a} e^{r_n} \cos \phi_n(\eta)$. Every amplified mode n of the field (6) takes the form of a product of a function of time and a (random, operator-valued) function of spatial coordinates; the mode acquires a standing-wave pattern. The periodic dependence $\cos \phi_n(\eta)$ will be further discussed below.

It is clearly seen from the fundamental equations (10), (11), (14) that the final results depend only on $a(\eta)$. Equations do not ask us the names of our favorite cosmological prejudices, they ask us about the pump field $a(\eta)$. Conversely, from the measured relic

gravitational waves, we can deduce the behaviour of $a(\eta)$, which is essentially the purpose of detecting the relic gravitons.

III. COSMOLOGICAL PUMP FIELD

With the chosen initial conditions, the final numerical results for relic gravitational waves depend on the concrete behaviour of the pump field represented by the cosmological scale factor $a(\eta)$. We know a great deal about $a(\eta)$. We know that $a(\eta)$ behaves as $a(\eta) \propto \eta^2$ at the present matter-dominated stage. We know that this stage was preceded by the radiation-dominated stage $a(\eta) \propto \eta$. At these two stages of evolution the functions $a(\eta)$ are simple power-law functions of η . What we do not know is the function $a(\eta)$ describing the initial stage of expansion of the very early Universe, that is, before the era of primordial nucleosynthesis. It is convenient to parameterize $a(\eta)$ at this initial stage also by power-law functions of η . First, this is a sufficiently broad class of functions, which, in addition, allows us to find exact solutions to our fundamental equations. Second, it is known [1] that the pump fields $a(\eta)$ which have power-law dependence in terms of η , produce gravitational waves with simple power-law spectra in terms of ν . These spectra are easy to analyze and discuss in the context of detection.

We model cosmological expansion by several successive eras. Concretely, we take $a(\eta)$ at the initial stage of expansion (i -stage) as

$$a(\eta) = l_o |\eta|^{1+\beta}, \quad (18)$$

where η grows from $-\infty$, and $1 + \beta < 0$. We will show later how the available observational data constrain the parameters l_o and β . The i -stage lasts up to a certain $\eta = \eta_1$, $\eta_1 < 0$. To make our analysis more general, we assume that the i -stage was followed by some interval of the z -stage (z from Zeldovich). It is known that an interval of evolution governed by the most “stiff” matter (effective equation of state $p = \epsilon$) advocated by Zeldovich, leads to a relative increase of gravitational wave amplitudes [1]. It is also known that the requirement of consistency of the graviton production with the observational restrictions does not allow the “stiff” matter interval to be too much long [1], [10]. However, we want to investigate any interval of cosmological evolution that can be consistently included. In fact, the z -stage of expansion that we include is quite general. It can be governed by a “stiffer than radiation” [11] matter, as well as by a “softer than radiation” matter. It can also be simply a part of the radiation-dominated era. Concretely, we take $a(\eta)$ at the interval of time from η_1 to some η_s (z -stage) in the form

$$a(\eta) = l_o a_z (\eta - \eta_p)^{1+\beta_s}, \quad (19)$$

where $1 + \beta_s > 0$. For the particular choice $\beta_s = 0$, the z -stage reduces to an interval of expansion governed by the radiation-dominated matter. Starting from η_s and up to η_2 the Universe was governed by the radiation-dominated matter (e -stage). So, at this interval of evolution, we take the scale factor in the form

$$a(\eta) = l_o a_e (\eta - \eta_e). \quad (20)$$

And, finally, from $\eta = \eta_2$ the expansion went over into the matter-dominated era (m -stage):

$$a(\eta) = l_o a_m (\eta - \eta_m)^2. \quad (21)$$

A link between the arbitrary constants participating in Eqs. (18) - (21) is provided by the conditions of continuous joining of the functions $a(\eta)$ and $a'(\eta)$ at points of transitions η_1, η_s, η_2 .

We denote the present time by η_R (R from reception). This time is defined by the observationally known value of the present-day Hubble parameter $H(\eta_R)$ and Hubble radius $l_H = c/H(\eta_R)$. For numerical estimates we will be using $l_H \approx 2 \times 10^{28}$ cm. It is convenient to choose $\eta_R - \eta_m = 1$, so that $a(\eta_R) = 2l_H$. The ratio

$$a(\eta_R)/a(\eta_2) \equiv \zeta_2$$

is believed to be around $\zeta_2 = 10^4$. We also denote

$$a(\eta_2)/a(\eta_s) \equiv \zeta_s, \quad a(\eta_s)/a(\eta_1) \equiv \zeta_1.$$

With these definitions, all the constants participating in Eqs. (18) - (21) (except parameters β and β_s which should be chosen from other considerations) are being expressed in terms of l_H, ζ_2, ζ_s , and ζ_1 . For example,

$$|\eta_1| = \frac{|1 + \beta|}{2\zeta_2^{\frac{1}{2}} \zeta_s \zeta_1^{\frac{1}{1+\beta_s}}}.$$

The important constant l_o is expressed as

$$l_o = b l_H \zeta_2^{\frac{\beta-1}{2}} \zeta_s^\beta \zeta_1^{\frac{\beta-\beta_s}{1+\beta_s}}, \quad (22)$$

where $b \equiv 2^{2+\beta}/|1 + \beta|^{1+\beta}$. Note that $b = 1$ for $\beta = -2$. [This expression for l_o may help to relate formulas written here with the equivalent treatment [19] which was given in slightly different notations.] The sketch of the entire evolution $a(\eta)$ is given in *Fig.4*.

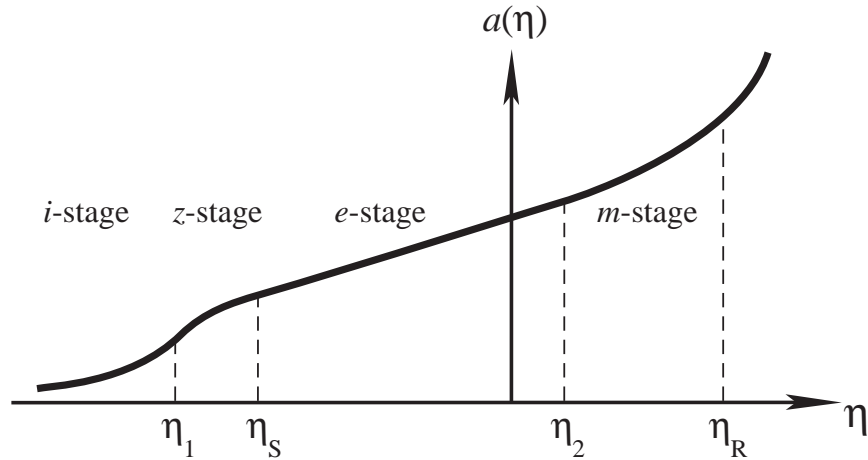


Fig. 4. Scale factor $a(\eta)$.

We work with the spatially-flat models (4). At every instant of time, the energy density $\epsilon(\eta)$ of matter driving the evolution is related with the Hubble radius $l(\eta)$ by

$$\kappa\epsilon(\eta) = \frac{3}{l^2(\eta)}, \quad (23)$$

where $\kappa = 8\pi G/c^4$. For the case of power-law scale factors $a(\eta) \propto \eta^{1+\beta}$, the effective pressure $p(\eta)$ of the matter is related with the $\epsilon(\eta)$ by the effective equation of state

$$p = \frac{1 - \beta}{3(1 + \beta)}\epsilon. \quad (24)$$

For instance, $p = 0$ for $\beta = 1$, $p = \frac{1}{3}\epsilon$ for $\beta = 0$, $p = -\epsilon$ for $\beta = -2$, and so on. Each interval of the evolution (18)-(21) is governed by one of these equations of state.

In principle, the function $a(\eta)$ could be even more complicated than the one that we consider. It could even include an interval of the early contraction, instead of expansion, leading to the ‘‘bounce’’ of the scale factor. In case of a decreasing $a(\eta)$ the gravitational-wave equation can still be analyzed and the amplification is still effective [1]. However, the Einstein equations for spatially-flat models do not permit a regular ‘‘bounce’’ of $a(\eta)$ (unless ϵ vanishes at the moment of ‘‘bounce’’). Possibly, a ‘‘bounce’’ solution can be realized in alternative theories, such, for example, as string-motivated cosmologies [13]. For a recent discussion of spectral slopes of gravitational waves produced in ‘‘bounce’’ cosmologies, see [14].

IV. SOLVING GRAVITATIONAL WAVE EQUATIONS

The evolution of the scale factor $a(\eta)$ given by Eqs. (18) - (21) and sketched in *Fig.4* allows us to calculate the function a'/a . This function is sketched in *Fig.5*. In all the theoretical generality, the left-hand-side of the barrier in *Fig.5* could also consist of several pieces, but we do not consider this possibility here. The graph also shows the important wave numbers n_H , n_2 , n_s , n_1 . The n_H marks the wave whose today’s wavelength $\lambda(\eta_R) = 2\pi a(\eta_R)/n_H$ is equal to the today’s Hubble radius l_H . With our parametrization $a(\eta_R) = 2l_H$, this wavenumber is $n_H = 4\pi$. The n_2 marks the wave whose wavelength $\lambda(\eta_2) = 2\pi a(\eta_2)/n_2$ at $\eta = \eta_2$ is equal to the Hubble radius $l(\eta_2)$ at $\eta = \eta_2$. Since $\lambda(\eta_R)/\lambda(\eta_2) = (n_2/n_H)[a(\eta_R)/a(\eta_2)]$ and $l(\eta_R)/l(\eta_2) = [a(\eta_R)/a(\eta_2)][a(\eta_R)/a(\eta_2)]^{1/2}$, this gives us $n_2/n_H = [a(\eta_R)/a(\eta_2)]^{1/2} = \zeta_2^{1/2}$. Working out in a similar fashion other ratios, we find

$$\frac{n_2}{n_H} = \zeta_2^{\frac{1}{2}}, \quad \frac{n_s}{n_2} = \zeta_s, \quad \frac{n_1}{n_s} = \zeta_1 \frac{1}{1+\beta_s}. \quad (25)$$

Solutions to the gravitational wave equations exist for any $a(\eta)$. At intervals of power-law dependence $a(\eta)$, solutions to Eq. (11) have simple form of the Bessel functions. We could have found piece-wise exact solutions to Eq. (11) and join them in the transition points. However, we will use a much simpler treatment which is sufficient for our purposes. We know that the squeeze parameter r_n stays constant in the short-wavelength regimes and grows according to Eq. (16) in the long-wavelength regime. All modes start in the vacuum state, that is, $r_n = 0$ initially. After the end of amplification, the accumulated value (17) stays constant up to today. To find today’s value of e^{r_n} we need to calculate

the ratio $a_{**}(n)/a_*(n)$. For every given n , the quantity a_* is determined by the condition $\lambda(\eta_*) = l(\eta_*)$, whereas a_{**} is determined by the condition $\lambda(\eta_{**}) = l(\eta_{**})$.

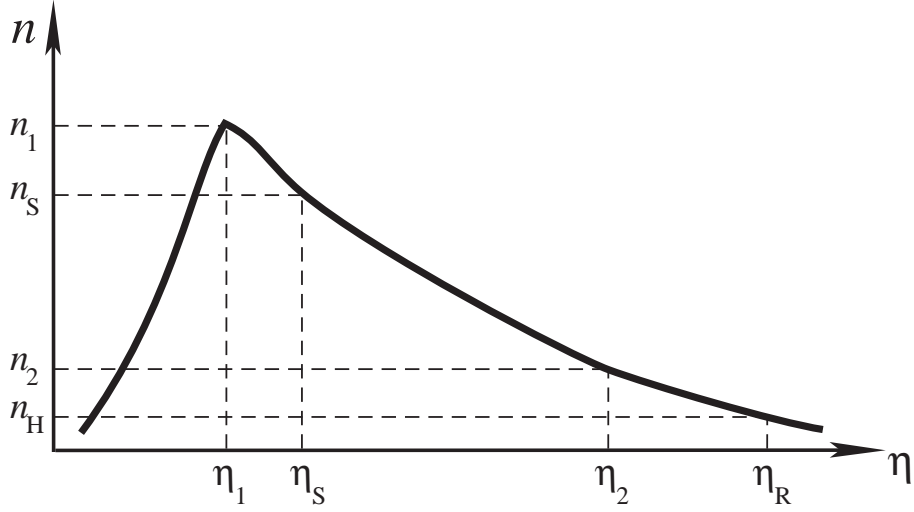


Fig. 5. Function $\frac{a'}{a}$ for the scale factor from Fig. 4.

Let us start from the mode $n = n_1$. For this wave number we have $a_* = a_{**} = a(\eta_1)$, and therefore $r_{n_1} = 0$. The higher frequency modes $n > n_1$ (above the barrier in Fig.5) have never been in the amplifying regime, so we can write

$$e^{r_n} = 1, \quad n \geq n_1. \quad (26)$$

Let us now consider the modes n in the interval $n_1 \geq n \geq n_s$. For a given n we need to know $a_*(n)$ and $a_{**}(n)$. Using Eq. (18) one finds $a_*(n)/a_*(n_1) = (n_1/n)^{1+\beta}$, and using Eq. (19) one finds $a_{**}(n)/a_{**}(n_s) = (n_s/n)^{1+\beta_s}$. Therefore, one finds

$$\frac{a_{**}(n)}{a_*(n)} = \frac{a_{**}(n_s)}{a_*(n_1)} \left(\frac{n_s}{n}\right)^{1+\beta_s} \left(\frac{n}{n_1}\right)^{1+\beta}.$$

Since $a_{**}(n_s) = a(\eta_s)$, $a_*(n_1) = a(\eta_1)$, and $a(\eta_s)/a(\eta_1) = \zeta_1 = (n_1/n_s)^{1+\beta_s}$, we arrive at

$$\frac{a_{**}(n)}{a_*(n)} = \left(\frac{n}{n_1}\right)^{\beta-\beta_s}.$$

Repeating this analysis for other intervals of the decreasing n , we come to the conclusion that

$$\begin{aligned} e^{r_n} &= \left(\frac{n}{n_1}\right)^{\beta-\beta_s}, \quad n_1 \geq n \geq n_s, \\ e^{r_n} &= \left(\frac{n}{n_s}\right)^\beta \left(\frac{n_s}{n_1}\right)^{\beta-\beta_s}, \quad n_s \geq n \geq n_2, \\ e^{r_n} &= \left(\frac{n}{n_2}\right)^{\beta-1} \left(\frac{n_2}{n_1}\right)^\beta \left(\frac{n_s}{n_1}\right)^{-\beta_s}, \quad n_2 \geq n \geq n_H. \end{aligned} \quad (27)$$

The mnemonic rule of constructing e^{r_n} at successive intervals of decreasing n is simple. If the interval begins at n_x , one takes $(n/n_x)^{\beta_* - \beta_{**}}$ and multiples with $e^{r_{n_x}}$, that is, with the previous interval's value e^{r_n} calculated at the end of that interval n_x . For the function a'/a that we are working with, the β_* is always β , whereas the β_{**} takes the values $\beta_s, 0, 1$ at the successive intervals.

The modes with $n < n_H$ are still in the long-wavelength regime. For these modes, we should take $a(\eta_R)$ instead of $a_{**}(n)$. Combining with $a_*(n)$, we find

$$e^{r_n} = \left(\frac{n}{n_H}\right)^{\beta+1} \left(\frac{n_H}{n_2}\right)^{\beta-1} \left(\frac{n_2}{n_1}\right)^{\beta} \left(\frac{n_s}{n_1}\right)^{-\beta_s}, \quad n \leq n_H. \quad (28)$$

Formulas (26) - (28) give approximate values of r_n for all n . The factor e^{r_n} is $e^{r_n} \geq 1$ for $n \leq n_1$, and $e^{r_n} \gg 1$ for $n \ll n_1$. This factor determines the mean square amplitude of the gravitational waves.

The mean value of the field h_{ij} is zero at every moment of time η and in every spatial point \mathbf{x} : $\langle 0|h_{ij}(\eta, \mathbf{x})|0\rangle = 0$. The variance

$$\langle 0|h_{ij}(\eta, \mathbf{x})h^{ij}(\eta, \mathbf{x})|0\rangle \equiv \langle h^2 \rangle$$

is not zero, and it determines the mean square amplitude of the generated field - the quantity of interest for the experiment. Taking the product of two expressions (6) one can show that

$$\langle h^2 \rangle = \frac{C^2}{2\pi^2} \int_0^\infty n \sum_{s=1}^2 |h_n^s(\eta)|^2 dn \equiv \int_0^\infty h^2(n, \eta) \frac{dn}{n}. \quad (29)$$

Using the representation (7), (8) in Eq. (29) one can also write

$$\langle h^2 \rangle = \frac{C^2}{\pi^2 a^2} \int_0^\infty n dn (\cosh 2r_n + \cos 2\phi_n \sinh 2r_n). \quad (30)$$

We can now consider the present era and use the fact that e^{r_n} are large numbers for all n in the interval of our interest $n_1 \geq n \geq n_H$. Then, we can derive

$$h(n, \eta) \approx \frac{C}{\pi} \frac{1}{a(\eta_R)} n e^{r_n} \cos \phi_n(\eta) = 8\sqrt{\pi} \left(\frac{l_{Pl}}{l_H}\right) \left(\frac{n}{n_H}\right) e^{r_n} \cos \phi_n(\eta). \quad (31)$$

The quantity $h(n, \eta)$ is the dimensionless spectral amplitude of the field whose numerical value is determined by the calculated squeeze parameter r_n . The oscillatory factor $\cos \phi_n(\eta)$ reflects the squeezing (standing wave pattern) acquired by modes with $n_1 > n > n_H$. For modes with $n < n_H$ this factor is approximately 1. For high-frequency modes $n \gg n_H$ one has $\phi_n(\eta) \approx n(\eta - \eta_n) \gg 1$, so that $h(n, \eta)$ makes many oscillations while the scale factor $a(\eta)$ is practically fixed at $a(\eta_R)$.

The integral (30) extends formally from 0 to ∞ . Since $r_n \approx 0$ for $n \geq n_1$, the integral diverges at the upper limit. This is a typical ultra-violet divergence. It should be discarded (renormalized to zero) because it comes from the modes which have always been in their vacuum state. At the lower limit, the integral diverges, if $\beta \leq -2$. This is an infra-red divergence which comes from the assumption that the amplification process has started from infinitely remote time in the past. One can deal with this divergence either by introducing a lower frequency cut-off (equivalent to the finite duration of the amplification) or by

considering only the parameters $\beta > -2$, in which case the integral is convergent at the lower limit. It appears that the available observational data (see below) favour this second option. The particular case $\beta = -2$ corresponds to the de Sitter evolution $a(\eta) \propto |\eta|^{-1}$. In this case, the $h(n)$ found in Eqs. (31), (28) does not depend on n . This is known as the Harrison-Zeldovich, or scale-invariant, spectrum.

An alternative derivation of the spectral amplitude $h(n)$ uses the approximate solutions (12), (13) to the wave equation (11). This method gives exactly the same, as in Eqs. (31), (26) - (28) numerical values of $h(n)$, but does not reproduce the oscillatory factor $\cos \phi_n(\eta)$.

One begins with the initial spectral amplitude $h_i(n)$ defined by quantum normalization: $h_i(n) = 8\sqrt{\pi}(l_{Pl}/\lambda_i)$. This is the amplitude of the mode n at the moment η_* of entering the long wavelength regime, i.e. when the mode's wavelength λ_i is equal to the Hubble radius $l(\eta_*)$. For λ_i one derives

$$\lambda_i = \frac{1}{b} l_o \left(\frac{n_H}{n} \right)^{2+\beta}. \quad (32)$$

Thus, we have

$$h_i(n) = A \left(\frac{n}{n_H} \right)^{2+\beta}, \quad (33)$$

where A denotes the constant

$$A = b8\sqrt{\pi} \frac{l_P l}{l_o}. \quad (34)$$

The numbers $h_i(n)$ are defined at the beginning of the long-wavelength regime. In other words, they are given along the left-hand-side slope of the barrier in *Fig.5*. We want to know the final numbers (spectral amplitudes) $h(n)$ which describe the field today, at η_R .

According to the dominant solution $h_n(\eta) = const$ of the long-wavelength regime (see Eq. (15)), the initial amplitude $h_i(n)$ stays practically constant up to the end of the long-wavelength regime at η_{**} , that is, up to the right-hand-side slope of the barrier. [The second term in Eq. (13) could be important only at the z -stage and only for parameters $\beta_s \leq -(1/2)$, which correspond to the effective equations of state $p \geq \epsilon$. In order to keep the analysis simple, we do not consider those cases.] After the completion of the long-wavelength regime, the amplitudes decrease adiabatically in proportion to $1/a(\eta)$, up to the present time. Thus, we have

$$h(n) = A \left(\frac{n}{n_H} \right)^{2+\beta} \frac{a_{**}(n)}{a(\eta_R)}. \quad (35)$$

Let us start from the lower end of the spectrum, $n \leq n_H$, and go upward in n . The modes $n \leq n_H$ have not started yet the adiabatic decrease of the amplitude, so we have

$$h(n) = A \left(\frac{n}{n_H} \right)^{2+\beta}, \quad n \leq n_H. \quad (36)$$

Now consider the interval $n_2 \geq n \geq n_H$. At this interval, the $a_{**}(n)/a(\eta_R)$ scales as $(n_H/n)^2$, so we have

$$h(n) = A \left(\frac{n}{n_H} \right)^\beta, \quad n_2 \geq n \geq n_H. \quad (37)$$

At the interval $n_s \geq n \geq n_2$ the ratio $a_{**}(n)/a(\eta_R) = [a_{**}(n)/a(\eta_2)][a(\eta_2)/a(\eta_R)]$ scales as $(n_2/n)(n_H/n_2)^2$, so we have

$$h(n) = A \left(\frac{n}{n_H} \right)^{1+\beta} \frac{n_H}{n_2}, \quad n_s \geq n \geq n_2. \quad (38)$$

Repeating the same analysis for the interval $n_1 \geq n \geq n_s$ we find

$$h(n) = A \left(\frac{n}{n_H} \right)^{1+\beta-\beta_s} \left(\frac{n_s}{n_H} \right)^{\beta_s} \frac{n_H}{n_2}, \quad n_1 \geq n \geq n_s. \quad (39)$$

It is seen from Eq. (39) that an interval of the z -stage with $\beta_s < 0$ (the already imposed restrictions require also $(-1/2) < \beta_s$) bends the spectrum $h(n)$ upwards, as compared with Eq. (38), for larger n . If one recalls the relationship (22) between l_o and l_H and uses (27), (28) in Eq. (31) one arrives exactly at Eqs. (36)-(39) up to the oscillating factor $\cos \phi_n(\eta)$.

Different parts of the barrier in *Fig.5* are responsible for amplitudes and spectral slopes at different intervals of n . The sketch of the generated spectrum $h(n)$ in conjunction with the form of the barrier is shown in *Fig.6*.

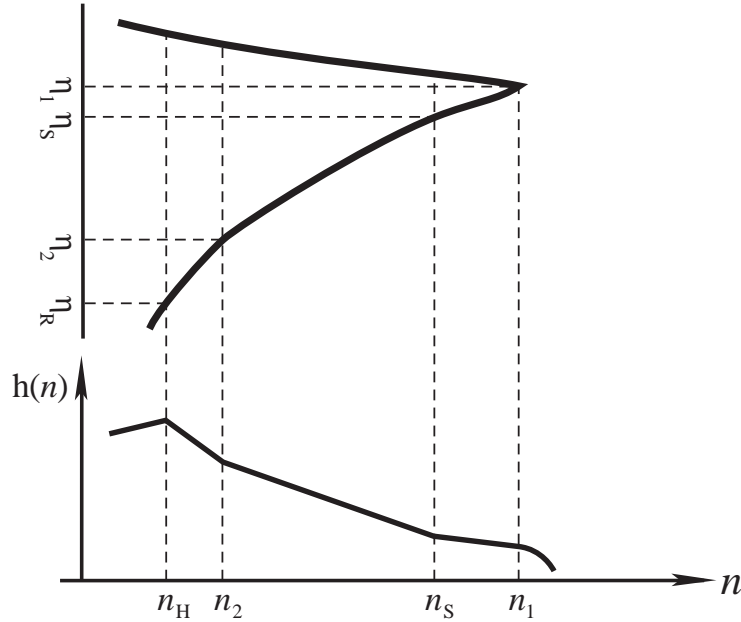


Fig. 6. Amplitudes and spectral slopes of $h(n)$ are determined by different parts of the barrier a'/a .

The present day frequency of the oscillating modes, measured in Hz , is defined as $\nu = cn/2\pi a(\eta_R)$. The lowest frequency (Hubble frequency) is $\nu_H = c/l_H$. For numerical estimates we will be using $\nu_H \approx 10^{-18} Hz$. The ratios of n are equal to the ratios of ν , so that, for example, $n/n_H = \nu/\nu_H$. For high-frequency modes we will now often use the ratios of ν instead of ratios of n .

In addition to the spectral amplitudes $h(n)$ the generated field can be also characterized by the spectral energy density parameter $\Omega_g(n)$. The energy density ϵ_g of the gravitational wave field is

$$\kappa\epsilon_g = \frac{1}{4}h_{,0}^{ij}h_{ij,0} = \frac{1}{4a^2}h^{ij'}h_{ij}'.$$

The mean value $\langle 0|\epsilon_g(\eta, \mathbf{x})|0\rangle$ is given by

$$\kappa\langle\epsilon_g\rangle = \frac{1}{4a^2} \frac{C^2}{2\pi^2} \int_0^\infty n \sum_{s=1}^2 |\dot{h}_n^{s'}(\eta)|^2 dn. \quad (40)$$

For high-frequency modes, it is only the factor $e^{\pm inn}$ that needs to be differentiated by η . After averaging out the oscillating factors, one gets $|\dot{h}_n^{s'}|^2 = n^2 |\dot{h}_n^s|^2$, so that

$$\kappa\langle\epsilon_g\rangle = \frac{1}{4a^2} \int_0^\infty n^2 h^2(n) \frac{dn}{n}. \quad (41)$$

In fact, the high-frequency approximation, that has been used, permits integration over lower n only up to n_H . And the upper limit, as was discussed above, is in practice n_1 , not infinity. The parameter Ω_g is defined as $\Omega_g = \langle\epsilon_g\rangle/\epsilon$, where ϵ is given by Eq. (23) (critical density). So, we derive

$$\Omega_g = \int_{n_H}^{n_1} \Omega_g(n) \frac{dn}{n} = \int_{\nu_H}^{\nu_1} \Omega_g(\nu) \frac{d\nu}{\nu}$$

and

$$\Omega_g(\nu) = \frac{\pi^2}{3} h^2(\nu) \left(\frac{\nu}{\nu_H} \right)^2. \quad (42)$$

The dimensionless quantity $\Omega_g(\nu)$ is useful because it allows us to quickly evaluate the cosmological importance of the generated field in a given frequency interval. However, the primary and more universal concept is $h(\nu)$, not $\Omega_g(\nu)$. It is the field, not its energy density, that is directly measured by the gravity-wave detector. One should also note that some authors use quite a misleading definition $\Omega_g(f) = (1/\rho_c)(d\rho_{gw}/d \ln f)$ which suggests differentiation of the gravity-wave energy density by frequency. This would be incorrect and could cause disagreements in numerical values of Ω_g . Whenever we use $\Omega_g(\nu)$, we mean relationship (42); and for order of magnitude estimates one can use [1]:

$$\Omega_g(\nu) \approx h^2(\nu) \left(\frac{\nu}{\nu_H} \right)^2. \quad (43)$$

V. THEORETICAL AND OBSERVATIONAL CONSTRAINTS

The entire theoretical approach is based on the assumption that a weak quantized gravity-wave field interacts with a classical pump field. We should follow the validity of this approximation throughout the analysis. The pump field can be treated as a classical gravitational

field as long as the driving energy density ϵ is smaller than the Planck energy density, or, in other words, as long as the Hubble radius $l(\eta)$ is greater than the Planck length l_{Pl} . This is a restriction on the pump field, but it can be used as a restriction on the wavelength λ_i of the gravity-wave mode n at the time of entry the long-wavelength regime. If $l(\eta_*) > l_{Pl}$, then $\lambda_i > l_{Pl}$. The λ_i is given by Eq. (32). So, we need to ensure that

$$b \frac{l_{Pl}}{l_o} \left(\frac{\nu}{\nu_H} \right)^{2+\beta} < 1.$$

At the lowest-frequency end $\nu = \nu_H$ this inequality gives $b(l_{Pl}/l_o) < 1$. In fact, the observational constraints (see below) give a stronger restriction:

$$b \frac{l_{Pl}}{l_o} \approx 10^{-6}, \quad (44)$$

which we accept. Then, at the highest-frequency end $\nu = \nu_1$ we need to satisfy

$$\left(\frac{\nu_1}{\nu_H} \right)^{2+\beta} < 10^6. \quad (45)$$

Let us now turn to the generated spectral amplitudes $h(\nu)$. According to Eq. (36) we have $h(\nu_H) \approx b8\sqrt{\pi}(l_{Pl}/l_o)$. The measured microwave background anisotropies, which we discuss below, require this number to be at the level of 10^{-5} , which gives the already mentioned Eq. (44). The quantity $h(\nu_1)$ at the highest frequency ν_1 is given by Eq. (39):

$$h(\nu_1) = b8\sqrt{\pi} \frac{l_{Pl}}{l_o} \left(\frac{\nu_1}{\nu_H} \right)^{1+\beta-\beta_s} \left(\frac{\nu_s}{\nu_H} \right)^{\beta_s} \frac{\nu_H}{\nu_2}.$$

Using Eq. (22) this expression for $h(\nu_1)$ can be rewritten as

$$h(\nu_1) = 8\sqrt{\pi} \frac{l_{Pl}}{l_H} \frac{\nu_1}{\nu_H} = 8\sqrt{\pi} \frac{l_{Pl}}{\lambda_1}, \quad (46)$$

where $\lambda_1 = c/\nu_1$. This last expression for $h(\nu_1)$ is not surprising: the modes with $\nu \geq \nu_1$ are still in the vacuum state, so the numerical value of $h(\nu_1)$ is determined by quantum normalization.

All the amplified modes have started with small initial amplitudes h_i , at the level of zero-point quantum fluctuations. These amplitudes are also small today, since the h_i could only stay constant or decrease. However, even these relatively small amplitudes should obey observational constraints. We do not want the Ω_g in the high-frequency modes, which might affect the rate of the primordial nucleosynthesis, to exceed the level of 10^{-5} . This means that $\Omega_g(\nu_1)$ cannot exceed the level of 10^{-6} or so. The use of Eq. (42) in combination with $\Omega_g(\nu_1) \approx 10^{-6}$ and $h(\nu_1)$ from Eq. (46), gives us the highest allowed frequency $\nu_1 \approx 3 \times 10^{10} Hz$. We will use this value of ν_1 in our numerical estimates. Returning with this value of ν_1 to Eq. (45) we find that parameter β can only be $\beta \leq -1.8$. We will be treating $\beta = -1.8$ as the upper limit for the allowed values of β .

We can now check whether the accepted parameters leave room for the postulated z -stage with $\beta_s < 0$. Using Eq. (22) we can rewrite Eq. (44) in the form

$$10^{-6} \frac{l_H}{l_{Pl}} = \left(\frac{\nu_1}{\nu_H} \right)^{-\beta} \left(\frac{\nu_1}{\nu_s} \right)^{\beta_s} \frac{\nu_2}{\nu_H}. \quad (47)$$

We know that $\nu_2/\nu_H = 10^2$ and ν_1/ν_s is not smaller than 1. Substituting all the numbers in Eq. (47) one can find that this equation cannot be satisfied for the largest possible $\beta = -1.8$. In the case $\beta = -1.9$, Eq. (47) is only marginally satisfied, in the sense that a significant deviation from $\beta_s = 0$ toward negative β_s can only last for a relatively short time. For instance, one can accommodate $\beta_s = -0.4$ and $\nu_s = 10^8 Hz$. On the other hand, if one takes $\beta = -2$, a somewhat longer interval of the z -stage with $\beta_s < 0$ can be included. For instance, Eq. (47) is satisfied if one accepts $\nu_s = 10^{-4} Hz$ and $\beta_s = -0.3$. This allows us to slightly increase $h(\nu)$ in the interval $\nu_s < \nu < \nu_1$, as compared with the values of $h(\nu)$ reached in the more traditional case $\beta = -2$, $\beta_s = 0$. In what follows, we will consider consequences of this assumption for the prospects of detection of the produced gravitational wave signal. Finally, let us see what the available information on the microwave background anisotropies [15], [16] allows us to conclude about the parameters β and l_o .

Usually, cosmologists operate with the spectral index n (not to be confused with the wave number n) of primordial cosmological perturbations. Taking into account the way in which the spectral index n is defined, one can relate n with the spectral index $\beta + 2$ that shows up in Eq. (36). The relationship between them is $n = 2\beta + 5$. This relationship is valid independently of the nature of cosmological perturbations. In particular, it is valid for density perturbations, in which case the $h(n)$ of Eq. (36) is the dimensionless spectral amplitude of metric perturbations associated with density perturbations. If primordial gravitational waves and density perturbations were generated by the mechanism that we discuss here (the assumption that is likely to be true) than the parameter β that participates in the spectral index is the same one that participates in the scale factor of Eq. (18). Primordial gravitational waves and primordial density perturbations with the same spectral index produce approximately the same lower-order multipole distributions of large-scale anisotropies.

The evaluation of the spectral index n of primordial perturbations have resulted in $n = 1.2 \pm 0.3$ [16] or even in a somewhat higher value. A recent analysis [17] of all available data favors $n = 1.2$ and the quadrupole contribution of gravitational waves twice as large as that of density perturbations. One can interpret these evaluations as indication that the true value of n lies somewhere near $n = 1.2$ (hopefully, the planned new observational missions will determine this index more accurately). This gives us the parameter β somewhere near $\beta = -1.9$. We will be using $\beta = -1.9$ in our estimates below, as the observationally preferred value. The parameter β can be somewhat larger than $\beta = -1.9$. However, as we already discussed, the value $\beta = -1.8$ ($n = 1.4$) is the largest one for which the entire approach is well posed. The Harrison-Zeldovich spectral index $n = 1$ corresponds to $\beta = -2$.

The observed quadrupole anisotropy of the microwave background radiation is at the level $\delta T/T \approx 10^{-5}$. The quadrupole anisotropy that would be produced by the spectrum (36) - (39) is mainly accounted for by the wave numbers near n_H . Thus, the numerical value of the quadrupole anisotropy produced by relic gravitational waves is approximately equal to A . According to general physical considerations and detailed calculations [18], the metric amplitudes of long-wavelength gravitational waves and density perturbations generated by the discussed amplification mechanism are of the same order of magnitude. Therefore, they contribute roughly equally to the anisotropy at lower multipoles. This gives us the estimate $A \approx 10^{-5}$, that we have already used in Eq. (44). It is not yet proven observationally that a

significant part of the observed anisotropies at lower multipoles is indeed provided by relic gravitational waves, but we can at least assume this with some degree of confidence. It is likely that the future measurements of the microwave background radiation will help us to verify this theoretical conclusion.

Combining all the evaluated parameters together, we show in *Fig.7* the expected spectrum of $h(\nu)$ for the case $\beta = -1.9$. A small allowed interval of the z -stage is also included. The intervals of the spectrum accessible to space-based and ground-based interferometers are indicated by vertical lines.

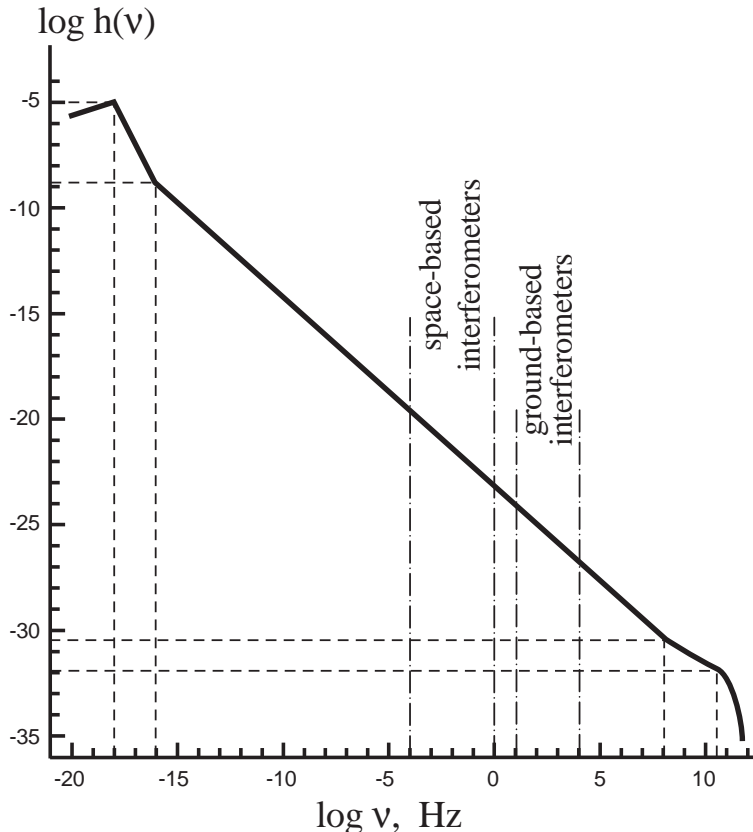


Fig. 7. Expected spectrum $h(\nu)$ for the case $\beta = -1.9$.

It is necessary to note [18], [19] that the confirmation of any $n > 1$ ($\beta > -2$) would mean that the very early Universe was not driven by a scalar field - the cornerstone of inflationary considerations. This is because the $n > 1$ ($\beta > -2$) requires the effective equation of state at the initial stage of expansion to be $\epsilon + p < 0$ (see Eq. (24)), but this cannot be accommodated by any scalar field with whichever scalar field potential. The available data do not prove yet that $n > 1$, but this possibility seems likely.

It is also necessary to say that a certain damage to gravitational wave research was inflicted by the so called “standard inflationary result”. The “standard inflationary result” predicts infinitely large amplitudes of density perturbations in the interval of spectrum with the Harrison-Zeldovich slope $n = 1$ ($\beta = -2$): $\delta\rho/\rho \propto 1/\sqrt{1-n}$. The metric (gravitational field) amplitudes of density perturbations are also predicted to be infinitely large, in the same proportion. Through the so-called “consistency relation” this divergence leads to the

vanishingly small amplitudes of relic gravitational waves. Thus, the “standard” inflationary theory predicts zero for relic gravitational waves; the spectrum similar in shape to the one shown in *Fig.7* would have been shifted down by many orders of magnitude. This prediction is hanging on the “standard inflationary result”, but the “result” itself is in a severe conflict not only with theory but with observations too: when the observers marginalize their data to $n = 1$ (enforce this value of n in data analysis) they find finite and small density perturbations instead of infinitely large perturbations predicted by inflationary theorists. [For analytical expressions of the “standard inflationary result” see any inflationary article, including recent reviews. For graphical illustration of the predicted divergent density perturbations and quadrupole anisotropies see, for example, [20]. For critical analysis and disagreement with the “standard inflationary result” see [18].] General relativity and quantum field theory do not produce the “standard inflationary result”, so we shall better return to what they say.

VI. DETECTABILITY OF RELIC GRAVITATIONAL WAVES

We switch now from cosmology to prospects of detecting the predicted relic gravitational waves. The ground-based [21]- [23] and space-based [24], [25] laser interferometers (see also [26]- [28]) will be in the focus of our attention. We use laboratory frequencies ν and intervals of laboratory time t ($cdt = a(\eta_R)d\eta$). Formulas (38) and (39), with $A = 10^{-5}$, $\nu_2/\nu_H = 10^2$, and the oscillating factor restored, can be written as

$$h(\nu, t) \approx 10^{-7} \cos[2\pi\nu(t - t_\nu)] \left(\frac{\nu}{\nu_H}\right)^{\beta+1}, \quad \nu_2 \leq \nu \leq \nu_s \quad (48)$$

and

$$h(\nu, t) \approx 10^{-7} \cos[2\pi\nu(t - t_\nu)] \left(\frac{\nu}{\nu_H}\right)^{1+\beta-\beta_s} \left(\frac{\nu_s}{\nu_H}\right)^{\beta_s}. \quad \nu_s \leq \nu \leq \nu_1 \quad (49)$$

where the deterministic (not random) constant t_ν does not vary significantly from one frequency to another at the intervals $\Delta\nu \approx \nu$. The explicit time dependence of the spectral variance $h^2(\nu, t)$ of the field, or, in other words, the explicit time dependence of the (zero-lag) temporal correlation function of the field at every given frequency, demonstrates that we are dealing with a non-stationary process (a consequence of squeezing and severe reduction of the phase uncertainty). We will first ignore the oscillating factor and will compare the predicted amplitudes with the sensitivity curves of advanced detectors. The potential reserve of improving the signal to noise ratio by exploiting the squeezing will be discussed later.

Let us start from the Laser Interferometer Space Antenna (LISA) [24]. The instrument will be most sensitive in the interval, roughly, from $10^{-3}Hz$ to $10^{-1}Hz$, and will be reasonably sensitive in a broader range, up to frequencies $10^{-4}Hz$ and $1Hz$. The sensitivity graph of LISA to a stochastic background is usually plotted under the assumption of a 1-year observation time, that is, the root-mean-square (r.m.s.) instrumental noise is being evaluated in frequency bins $\Delta\nu = 3 \times 10^{-8}Hz$ around each frequency ν . We need to rescale our predicted amplitude $h(\nu)$ to these bins.

The mean square amplitude of the gravitational wave field is given by the integral (29). Thus, the r.m.s. amplitude in the band $\Delta\nu$ centered at a given frequency ν is given by the expression

$$h(\nu, \Delta\nu) = h(\nu) \sqrt{\frac{\Delta\nu}{\nu}}. \quad (50)$$

We use Eqs. (48), (49) and calculate expression (50) assuming $\Delta\nu = 3 \times 10^{-8} Hz$. The results are plotted in *Fig.8*. Formula (48) has been used throughout the covered frequency interval for the realistic case $\beta = -1.9$ and for the extreme case $\beta = -1.8$. The line marked *z-model* describes the signal produced in the composite model with $\beta = -2$ up to $\nu_s = 10^{-4} Hz$ (formula (48)) and then followed by formula (49) with $\beta_s = -0.3$. This model gives the signal a factor of 3 higher at $\nu = 10^{-3} Hz$, than the model $\beta = -2$ extrapolated down to this frequency.

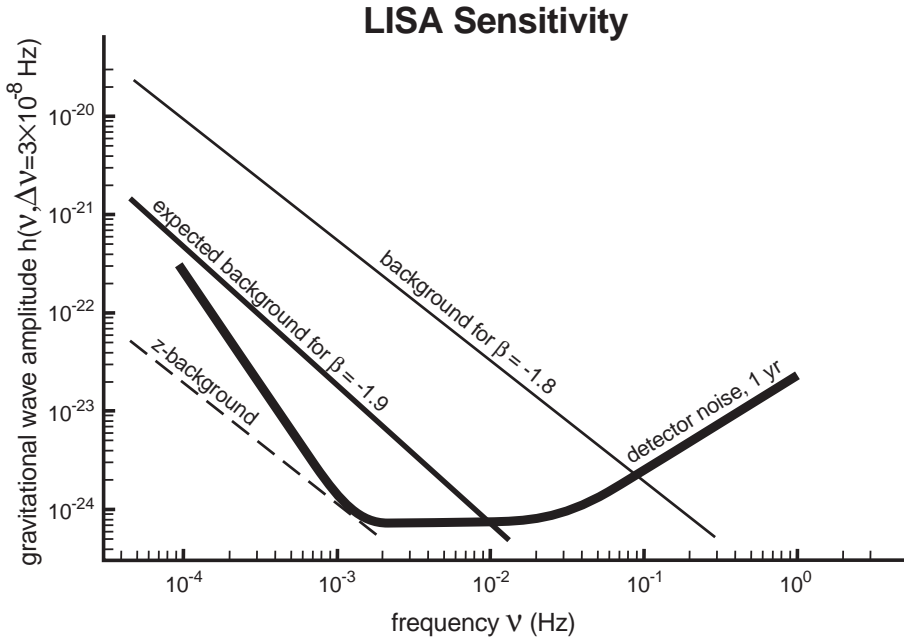


Fig. 8. Expected spectrum $\beta = -1.9$ and other possible spectra in comparison with the LISA sensitivity.

There is no doubt that the signal $\beta = -1.8$ would be easily detectable even with a single instrument. The signal $\beta = -1.9$ is marginally detectable, with the signal to noise ratio around 3 or so, in a quite narrow frequency interval near and above the frequency $3 \times 10^{-3} Hz$. However, at lower frequencies one would need to be concerned with the possible gravitational wave noise from unresolved binary stars in our Galaxy. The further improvement of the expected LISA sensitivity by a factor of 3 may prove to be crucial for a confident detection of the predicted signal with $\beta = -1.9$.

Let us now turn to the ground-based interferometers operating in the interval from $10 Hz$ to $10^4 Hz$. The best sensitivity is reached in the band around $\nu = 10^2 Hz$. We take this frequency as the representative frequency for comparison with the predicted signal. We will work directly in terms of the dimensionless quantity $h(\nu)$. If necessary, the r.m.s. amplitude per $Hz^{1/2}$ at a given ν can be found simply as $h(\nu)/\sqrt{\nu}$. The instrumental noise will also be quoted in terms of the dimensionless quantity $h_{ex}(\nu)$.

The expected sensitivity of the initial instruments at $\nu = 10^2 \text{ Hz}$ is $h_{ex} = 10^{-21}$ or better. The theoretical prediction at this frequency, following from (48), (49) with $\beta_s = 0$, is $h_{th} = 10^{-23}$ for $\beta = -1.8$, and $h_{th} = 10^{-25}$ for $\beta = -1.9$. Therefore, the gap between the signal and noise levels is from 2 to 4 orders of magnitude. The expected sensitivity of the advanced interferometers, such as LIGO-II [29], can be as high as $h_{ex} = 10^{-23}$. In this case, the gap vanishes for the $\beta = -1.8$ signal and reduces to 2 orders of magnitude for the $\beta = -1.9$ signal. *Fig.9* illustrates the expected signal in comparison with the LIGO-II sensitivity. Since the signal lines are plotted in terms of $h(\nu)$, the LISA sensitivity curve (shown for periodic sources) should be raised and adjusted in accordance with *Fig.8*.

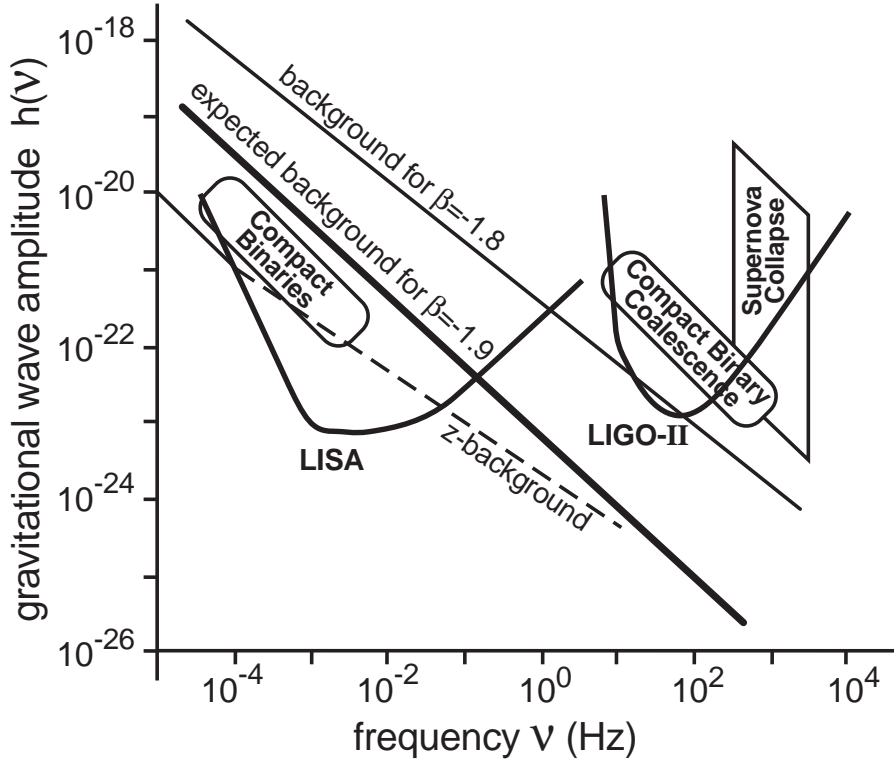


Fig. 9. Full spectrum $h(\nu)$ accessible to laser interferometers.

A signal below noise can be detected if the outputs of two or more detectors can be cross correlated. [For the early estimates of detectability of relic gravitational waves see [30].] The cross correlation will be possible for ground-based interferometers, several of which are currently under construction. The gap between the signal and the noise levels should be covered by a sufficiently long observation time τ . The duration τ depends on whether the signal has any temporal signature known in advance, or not. We start from the assumption that no temporal signatures are known in advance. In other words, we first ignore the squeezed nature of the relic background and work under the assumption that the squeezing cannot be exploited to our advantage.

The response of an instrument to the incoming radiation is $s(t) = F_{ij}h^{ij}$ where F_{ij} depends on the position and orientation of the instrument. Since the h^{ij} is a quantum-mechanical operator (see Eq. (6)) we need to calculate the mean value of a quadratic

quantity. The mean value of the cross correlation of responses from two instruments $\langle 0|s_1(t)s_2(t)|0\rangle$ will involve the overlap reduction function [31]- [34], which we assume to be not much smaller than 1 [33]. The signal to noise ratio S/N in the measurement of the amplitude of a signal with no specific known features increases as $(\tau\nu)^{1/4}$, where ν is some characteristic central frequency. If the signal has features known in advance and exploited by the matched filtering technique, the S/N increases as $(\tau\nu)^{1/2}$.

We apply the guaranteed law $(\tau\nu)^{1/4}$ to initial and advanced instruments at the representative frequency $\nu = 10^2 Hz$. This law requires a reasonably short time $\tau = 10^6$ sec in order to improve the S/N in initial instruments by two orders of magnitude and to reach the level of the signal with extreme spectral index $\beta = -1.8$. The longer integration time or a better sensitivity will make the S/N larger than 1. In the case of a realistic spectral index $\beta = -1.9$ the remaining gap of 4 orders of magnitude can be covered by the combination of a significantly better sensitivity and a longer observation time (not necessarily in one non-interrupted run). The sensitivity of the advanced laser interferometers, such as LIGO II, at the level $h_{ex} = 10^{-23}$ and the same observation time $\tau = 10^6$ sec would be sufficient for reaching the level of the predicted signal with $\beta = -1.9$.

An additional increase of S/N can be achieved if the statistical properties of the signal can be properly exploited. Squeezing is automatically present at all frequencies from ν_H to ν_1 . The squeeze parameter r is larger in gravitational waves of cosmological scales, and possibly the periodic structure in Eq. (31) can be better revealed at those scales. However, we are interested here in frequencies accessible to ground based interferometers, say, in the interval $30Hz - 100Hz$. If our intention were to monitor one given frequency ν from the beginning of its oscillating regime and up till now, then, in order to avoid the destructive interference from neighbouring modes during all that time, the frequency resolution of the instrument should have been incredibly narrow, of the order of $10^{-18}Hz$. Certainly, this is not something what we can, or intend to do. Although the amplitudes of the waves have adiabatically decreased and their frequencies redshifted since the beginning of their oscillating regime, the general statistical properties of the discussed signal are essentially the same now as they were 10 years after the Big Bang or will be 1 million years from now.

The periodic structure (48) may survive at some level in the instrumental window of sensitivity from ν_{min} (minimal frequency) to ν_{max} (maximal frequency). The mean square value of the field in this window is

$$\int_{\nu_{min}}^{\nu_{max}} h^2(\nu, t) \frac{d\nu}{\nu} = 10^{-14} \frac{1}{\nu_H^{2\beta+2}} \int_{\nu_{min}}^{\nu_{max}} \cos^2[2\pi\nu(t - t_\nu)] \nu^{2\beta+1} d\nu . \quad (51)$$

Because of the strong dependence of the integrand on frequency, $\nu^{-2.6}$ or $\nu^{-2.8}$, the value of the integral (51) is determined by its lower limit. Apparently, the search through the data should be based on the periodic structure that may survive at $\nu = \nu_{min}$. As an illustration, one can consider such a narrow interval $\Delta\nu = \nu_{max} - \nu_{min}$ that the integral (51) can be approximated by the formula

$$\int_{\nu_{min}}^{\nu_{max}} h^2(\nu, t) \frac{d\nu}{\nu} \approx 10^{-14} \left(\frac{\nu_{min}}{\nu_H} \right)^{2\beta+2} \left(\frac{\Delta\nu}{\nu_{min}} \right) \cos^2[2\pi\nu_{min}(t - t_{min})] .$$

Clearly, the correlation function is strictly periodic and its structure is known in advance, in contrast to other possible signals. This is a typical example of using the a priori information.

Ideally, the gain in S/N can grow as $(\tau\nu_{min})^{1/2}$. This would significantly reduce the required observation time τ . For a larger $\Delta\nu$, even an intermediate gain between the guaranteed law $(\tau\nu)^{1/4}$ and the law $(\tau\nu)^{1/2}$, adequate for the matched filtering technique, would help. This could potentially make the signal with $\beta = -1.9$ measurable even by the initial laser interferometers. A straightforward application of (51) for exploiting the squeezing may not be possible, as argued in the recent study [35], but more sophisticated methods are not excluded.

For frequency intervals covered by bar detectors and electromagnetic detectors, the expected results follow from the same formulas (48), (49) and have been briefly discussed elsewhere [30], [19].

VII. CONCLUSION

It would be strange, if the predicted signal at the level corresponding to $\beta = -1.9$ were not seen by the instruments capable of its detection. There is not so many cosmological assumptions involved in the derivation, that could prove wrong, thus invalidating our predictions. On the other hand, it would be even more strange (and even more interesting) if the relic gravitational waves were detected at the level above the $\beta = -1.8$ line. This would mean that there is something fundamentally wrong in our basic cosmological premises. To summarise, it is quite possible that the detection of relic (squeezed) gravitational waves may be awaiting only the first generation of sensitive instruments and an appropriate data processing strategy.

VIII. ACKNOWLEDGEMENTS

I appreciate the help of M. V. Prokhorov in preparation of the figures.

-
- [1] L. P. Grishchuk, Zh. Eksp. Teor. Fiz. **67**, 825 (1974) [JETP **40**, 409 (1975)]; Ann. NY Acad. Sci. **302**, 439 (1977); Uspekhi Fiz. Nauk. **156**, 297 (1988) [Sov. Phys.-Uspekhi. **31**, 940 (1988)].
 - [2] K. S. Thorne, in *300 Years of Gravitation*, eds. S. W. Hawking and W. Israel (Cambridge: CUP) 1987, p. 330.
 - [3] K. S. Thorne, in *Particle and Nuclear Astrophysics and Cosmology in the Next Millenium*, eds. E. Kolb and R. Peccei (Singapore: World Scientific) 1995, p. 160.
 - [4] B. F. Schutz, Class. Quant. Grav. **16**, A131 (1999).
 - [5] P. L. Knight, in *Quantum Fluctuations*, Eds. S. Reynaud, E. Giacobino, and J. Zinn-Justin, (Elsevier Science) 1997, p. 5.
 - [6] L. P. Grishchuk and Yu. V. Sidorov, Class. Quant. Grav. **6**, L161 (1989); Phys. Rev. **D42**, 3413 (1990).
 - [7] L. P. Grishchuk, in *Workshop on Squeezed States and Uncertainty Relations*, NASA Conf. Publ. **3135**, 1992, p. 329; Class. Quant. Grav. **10**, 2449 (1993); in *Quantum Fluctuations*, Eds. S. Reynaud, E. Giacobino, and J. Zinn-Justin, (Elsevier Science) 1997, p. 541.
 - [8] L. D. Landau and E. M. Lifshitz, *The Classical Theory of Fields* (New York: Pergamon) 1975.

- [9] W. Schleich and J. A. Wheeler, *J. Opt. Soc. Am* **B4**, 1715 (1987); W. Schleich *et. al.*, *Phys. Rev.* **A40**, 7405 (1989).
- [10] Ya. B. Zeldovich and I. D. Novikov, *The Structure and Evolution of the Universe* (Chicago, IL: University of Chicago Press) 1983.
- [11] M. Giovannini, *Phys. Rev.* **D58**, 083504 (1998); Report hep-ph/9912480.
- [12] L. P. Grishchuk, Report gr-qc/9810055.
- [13] G. Veneziano, *Phys. Lett.* **B265**, 287 (1991); M. Gasperini and G. Veneziano, *Astropart. Phys.* **1**, 317 (1993); M. Gasperini and M. Giovannini, *Phys. Rev.* **D47**, 1519 (1993); M. Gasperini, Report hep-th/9607146.
- [14] T. Creighton, Report gr-qc/9907045.
- [15] G. F. Smoot *et. al.*, *Astroph. J.* **396**, L1 (1992).
- [16] C. L. Bennet *et. al.*, *Astroph. J.* **464**, L1 (1996).
- [17] A. Melchiori, M. V. Sazhin, V. V. Shulga, and N. Vittorio, *Astroph. J.* **518**, 562 (1999).
- [18] L. P. Grishchuk, *Phys. Rev.* **D50**, 7154 (1994); in *Current Topics in Astrofundamental Physics: Primordial Cosmology*, Eds. N. Sanchez and A. Zichichi, (Kluwer Academic) 1998, p. 539; Report gr-qc/9801011.
- [19] L. P. Grishchuk, *Class. Quant. Grav.* **14**, 1445 (1997).
- [20] J. Martin and D. J. Schwarz, Report astro-ph/9911225.
- [21] A. Abramovici *et. al.*, *Science* **256**, 325 (1992).
- [22] C. Bradaschia *et. al.*, *Nucl. Instrum. and Methods* **A289**, 518 (1990).
- [23] J. Hough and K. Danzmann *et. al.*, *GEO600 Proposal*, 1994.
- [24] P. Bender *et. al.* *LISA Pre-Phase A Report*, Second Edition, 1998
- [25] S. L. Larson, W. A. Hiscock. and R. W. Hellings, Report gr-qc/9909080.
- [26] *Gravitational Wave Experiments*, eds. E. Coccia, G. Pizzella, and F. Ronga (Singapore: World Scientific) 1995.
- [27] *Gravitational Waves: Sources and detection*, eds. I. Giufolini and F. Fiducaro (Singapore: World Scientific) 1997.
- [28] *Laser Interferometer Space Antenna*, ed. W. Folkner (AIP Conference Proceedings 456) 1998.
- [29] *LIGO II Conceptual Project Book*, LIGO-M990288-00-M.
- [30] L. P. Grishchuk, *Pis'ma Zh. Eks. Teor. Fiz.* **23**, 326 (1976) [*JETP Lett.* **23**, 293 (1976)].
- [31] P. F. Michelson, *Mon. Not. R. Astr. Soc.* **227**, 933 (1987).
- [32] N. L. Christensen, *Phys. Rev.* **D46**, 5250 (1992).
- [33] E. E. Flanagan, *Phys. Rev.* **D48**, 2389 (1993).
- [34] B. Allen, in *Relativistic Gravitation and Gravitational Radiation*, Eds. J-A. Marck and J-P. Lasota (CUP, 1997) p. 373.
- [35] B. Allen, E. E. Flanagan, and M. A. Papa. Report gr-qc/9906054.